JCI The Journal of Clinical Investigation

Marked and rapid effects of pharmacological HIF-2α antagonism on hypoxic ventilatory control

Xiaotong Cheng, … , Tammie Bishop, Peter J. Ratcliffe

J Clin Invest. 2020. https://doi.org/10.1172/JCI133194.

Research In-Press Preview Therapeutics

Graphical abstract

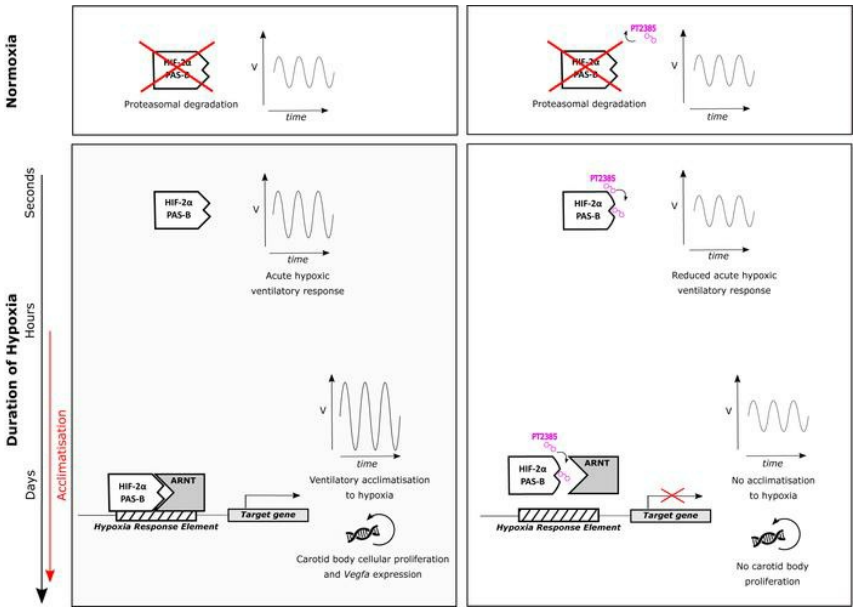

Find the latest version:

https://jci.me/133194/pdf

Marked and rapid effects of pharmacological HIF-2α antagonism on hypoxic ventilatory control

Xiaotong Cheng[1, 2], Maria Prange-Barczynska[1, 2], James W. Fielding[1, 2], Minghao Zhang[1], Alana L. Burrell[3], Joanna D. C. C. Lima[1], Luise Eckardt[1], Isobel L. A. Argles[1], Christopher W. Pugh[1], Keith J. Buckler[4], Peter A. Robbins[4], Emma J. Hodson[3], Richard K. Bruick[5], Lucy M. Collinson[3], Fraydoon Rastinejad[1], Tammie Bishop[1] and Peter J. Ratcliffe[1, 2, 3]

[1]Target Discovery Institute, University of Oxford, Oxford, UK

[2]Ludwig Institute for Cancer Research, University of Oxford, Oxford, UK

[3]The Francis Crick Institute, London, UK

[4]Department of Physiology, Anatomy and Genetics, University of Oxford, Oxford, UK

[5]Department of Biochemistry, University of Texas Southwestern Medical Center, Dallas, Texas, USA

Authorship note:

XC, MPB and JWF are joint first authors. TB and PJR are co-senior authors.

Correspondence to:

Tammie Bishop or Peter J. Ratcliffe

Target Discovery Institute,

Roosevelt Drive,

Oxford, OX3 7FZ, UK

Tel: +44-1865-612-680

tammie.bishop@ndm.ox.ac.uk; peter.ratcliffe@ndm.ox.ac.uk

Conflict of interest

RKB is employed by Peloton Therapeutics, Inc., a wholly-owned subsidiary of Merck & Co., Inc. (Kenilworth, New Jersey, USA). CWP and PJR are scientific co-founders of ReOx Ltd. (Oxford, UK), an Oxford University spin-off company.

Abstract

Hypoxia-inducible factor (HIF) is strikingly upregulated in many types of cancer and there is great interest in applying inhibitors of HIF as anti-cancer therapeutics. The most advanced of these are small molecules that target the HIF-2 isoform through binding the PAS-B domain of HIF-2α. These molecules are undergoing clinical trials with promising results in renal and other cancers where HIF-2 is considered to be driving growth. Nevertheless, a central question remains as to whether such inhibitors impact on physiological responses to hypoxia at relevant doses. Here we show that pharmacological HIF-2α inhibition with PT2385, at doses similar to those reported to inhibit tumour growth, rapidly impaired ventilatory responses to hypoxia, abrogating both ventilatory acclimatisation and carotid body cell proliferative responses to sustained hypoxia. Mice carrying a HIF-2α PAS-B S305M mutation that disrupts PT2385 binding, but not dimerisation with HIF-1β, did not respond to PT2385 indicating that these effects are on target. Furthermore, the finding of a hypomorphic ventilatory phenotype in untreated HIF-2α S305M mutant mice suggests a function for the HIF-2α PAS-B domain beyond heterodimerisation with HIF-1β. Although PT2385 was well-tolerated, the findings indicate the need for caution in patients who are dependent on hypoxic ventilatory drive.

Introduction

Hypoxia-inducible factors (HIFs) are transcriptional factors that mediate a wide range of adaptive responses to low oxygen and play a central role in the maintenance of oxygen homeostasis (reviewed in (1-3)). As disturbances of oxygen homeostasis are critical to many aspects of human disease, there is great interest in developing agents that modulate HIF pathways, and in defining the benefits and risks of their therapeutic use (4, 5).

The HIF DNA binding complex comprises an α/β heterodimer of basic helix-loop-helix (bHLH) PAS proteins. Oxygen-dependent activity of HIF is conveyed by the HIF-α subunit; in human cells there are three HIF-α isoforms, of which HIF-1α and HIF-2α are the most strongly expressed and best understood. In cancer, HIFs are frequently upregulated either by micro-environmental hypoxia within the tumour or by genetic connections to mutant oncogene or tumour suppressor pathways (reviewed in (1-3)). Thus, HIF constitutes a key 'growth support' pathway for cancer, enhancing oxygen delivery through angiogenesis and promoting a range of tumour-associated phenotypes. In some cancers, it has further been proposed that the activation of HIF is not just supporting tumour growth, but driving its progression. One example is clear cell renal cell carcinoma (ccRCC), the commonest form of human kidney cancer (6, 7). These tumours frequently manifest biallelic inactivation of the von Hippel-Lindau tumour suppressor pVHL, a ubiquitin E3 ligase that normally targets HIF-α for destruction in the presence of oxygen (reviewed in (6, 7)). Inactivation of pVHL leads to constitutive stabilisation of HIF-α in ccRCC. Interestingly, ccRCC commonly manifests a strong bias towards expression of HIF-2α and genetic interventions on HIF-2α in ccRCC cells grown as tumour xenografts suggest that this isoform is necessary and sufficient to drive ccRCC (8,

9). These findings have led to great interest in the development of therapeutic agents that antagonise HIFs, either specifically or generally, for the treatment of cancer.

The most advanced of these approaches is represented by molecules that specifically target a pocket in the PAS-B domain of HIF-2α to allosterically destabilise the heterodimeric complex involving HIF-2α with HIF-1β and hence inhibit HIF-2 transcriptional activity (10, 11). These antagonists have shown efficacy in preclinical models using ccRCC cell lines or patient-derived ccRCC xenografts (12-14) and in early phase clinical trials on therapy-resistant advanced ccRCC (15, 16). These molecules are also undergoing clinical trials in other cancers where the HIF-2α isoform is considered to be particularly important (17) and in ccRCC which is associated with inherited von Hippel-Lindau disease (18).

However, because HIF, including HIF-2, is involved in many aspects of normal physiology, a key question arises as to whether such agents affect the function of non-neoplastic tissues and, if so, at what dose and under which circumstances. One important response in which HIF, in particular HIF-2, has been implicated by genetic interventions is in the control of respiration by the carotid body (19-21). However, in common with most studies that deploy genetic inactivation technology, such studies generally aim to generate complete loss of a specific HIF-α protein in a specific cell type and do not necessarily mimic dose-dependent actions of a pharmaceutical agent that is applied systemically.

As interventions on the HIF system move forward through clinical trials, there is a pressing need to understand better their effects on systemic physiology. To that end, we have examined the effects of PT2385, one of the HIF-2α antagonists that shows clinical efficacy in ccRCC (15), on morphological changes and hypoxic ventilatory control that are mediated by the carotid body. We report that PT2385 blocks the proliferative and ultrastructural changes

in the cells within this organ that are observed in response to hypoxia. Enhanced ventilatory sensitivity to hypoxia was rapidly and severely ablated at the doses of PT2385 for which anti-tumour effects have been reported (14). These effects were not observed in recombinant mice containing a mutation in *Epas1* (the gene encoding HIF-2α), which largely ablates the binding of PT2385 to HIF-2α, indicating that they represent on-target effects of the molecule.

Results

Effects of PT2385 on ventilatory sensitivity to hypoxia

In response to breathing a hypoxic atmosphere, pulmonary ventilation increases rapidly within seconds, then more progressively over hours to days as hypoxia is sustained, a phenomenon that is termed ventilatory acclimatisation (22). These responses involve a progressive increase in ventilatory sensitivity to chemoreceptive stimuli in the carotid body. Because in clinical or physiological settings, such as chronic lung disease or altitude exposure, hypoxia is generally sustained, and because genetic studies have suggested an important role for HIF-2 in this setting (19, 20, 23, 24), we first studied the effects of PT2385 on ventilatory sensitivity in animals exposed to sustained hypoxia.

Male mice were treated by gavage with 3 or 10 mg kg^{-1} PT2385 (or vehicle alone) twice daily; doses that have been shown to be effective in reducing tumour size in ccRCC xenografts in mice (14). PT2385 was commenced 24 h prior to, and maintained throughout, the 7 d exposure of mice to hypoxia. To monitor changes in ventilatory sensitivity during this period, mice were removed from the normobaric altitude chamber, placed into the plethysmograph and allowed to equilibrate to normal air then subjected to defined acute (5 min) gas challenges (10 % oxygen alone, 10 % oxygen with 3 % carbon dioxide and 3 % carbon dioxide alone) prior to the start of the experiment and after 2, 5 and 7 d of sustained hypoxia. Acute (5 min) challenge with 10 % oxygen alone elicits a poorly sustained increase in ventilation due to hyperventilation-induced hypocapnia. Therefore, the challenge of 10 % oxygen with 3 % carbon dioxide (calculated to provide approximate compensation for hypocapnia) was used as the main test gas to approximate isocapnic hypoxia as described in (19, 20, 25). Ventilatory responses to all three gas challenges are shown in Figure 1, Table 1, Figure S1 and S2.

Progressive increases in ventilatory sensitivity were observed with sustained hypoxia in control mice treated with vehicle alone, with marked increases in responses to gas challenges after 2 d at 10 % oxygen that were further enhanced after 5 and 7 d at 10 % oxygen (Figure 1 and S1 open circles; Table 1). Strikingly, treatment with PT2385 at both 3 and 10 mg kg^{-1} doses essentially ablated these increases in ventilatory sensitivity (Figure 1 and S1, closed circles; Table 1). For example, acute ventilatory responses (AVRs) to 10 % oxygen with 3 % carbon dioxide after 7 d hypoxia were reduced from 9.22 ± 1.60 mL min^{-1} g^{-1} in vehicle-treated mice to 4.24 ± 0.90 mL min^{-1} g^{-1} in mice treated with 3 mg kg^{-1} PT2385, and were similar to those at baseline i.e. prior to sustained hypoxia (4.18 ± 0.43 mL min^{-1} g^{-1}). In the case of the 10 mg kg^{-1} dose, AVRs of mice treated with PT2385 and in 7 d hypoxia were lower than those at baseline (2.02 ± 0.62 versus 4.31 ± 0.73 mL min^{-1} g^{-1}). Similar observations were made when 10 % oxygen was used as the acute gas challenge although, as discussed above, these responses were less sustained (Table 1 and Figure S2). Interestingly, PT2385 treatment also reduced responses to 3 % carbon dioxide in this setting (Table 1). In humans, ventilatory acclimatisation to hypoxia is known to increase the sensitivity of the central chemoreflex response to carbon dioxide, so as to increase the slope of the relationship between minute ventilation and end-tidal carbon dioxide (26). Hence, the reduced sensitivity of PT2385-treated mice to carbon dioxide in this setting is also consistent with an action of PT2385 on ventilatory acclimatisation to hypoxia. In summary, these findings reveal that treatment with PT2385 exerts striking effects on ventilatory control, essentially ablating the enhanced ventilatory sensitivity, or ventilatory acclimatisation, that occurs during sustained exposure to hypoxia. We further sought to test whether PT2385 has similar effects on hypoxic ventilatory control in female mice compared to those observed in male mice. As with male

mice, ventilatory acclimatisation was abolished in female mice treated with either 3 or 10 mg kg^{-1} PT2385 (Figure S3 and Table S1).

Interestingly, neither 3 nor 10 mg kg^{-1} PT2385 treatment during sustained hypoxia significantly altered haematocrits in male or female mice compared to vehicle-treated control mice in hypoxia (Figure S4). This may be because the failure to acclimatise with PT2385 treatment results in greater hypoxaemia and a higher hypoxic drive on erythropoietin expression; indeed, 10 mg kg^{-1} PT2385 treatment over the equivalent time-course (8 d) in normoxic male mice does result in a significant reduction in haematocrits (Figure S4), in line with the anaemia observed in patients treated with PT2385 (15).

To pursue the effects on ventilatory acclimatisation further, we next tested whether PT2385 treatment could reverse enhanced ventilatory sensitivity that has already been established, either through prior exposure to sustained hypoxia or in the setting of pseudohypoxia following genetic inactivation of a negative regulator of HIF. To test the former, wild-type male mice were first exposed to 10 % oxygen for 7 d, after which they were treated with 10 mg kg^{-1} PT2385, or vehicle, twice daily and maintained in hypoxia (Figure 2A and B). Ventilatory sensitivity was measured using the same acute 5 min challenges with test gases as described above. PT2385 treatment progressively reversed enhanced ventilatory sensitivity, reducing the responses to those observed in unacclimatised mice within 24 h (Figure 2A and B). To test the effects of PT2385 in the setting of pseudohypoxic enhancement of ventilatory sensitivity, male mice with heterozygous inactivation of HIF prolyl hydroxylase 2 *(Phd2,* the principal PHD isoform which negatively regulates HIF (27, 28)) were treated with 10 mg kg^{-1} PT2385. As reported (20, 25), *Phd2*$^{+/-}$ mice displayed enhanced hypoxic ventilatory sensitivity compared with their wild-type littermates (Figure 2C and D). These responses were

also reduced by PT2385, although interestingly this appeared to require longer exposure to the compound. Whereas PT2385 completely reversed enhanced ventilatory sensitivity to environmental hypoxia within 24 h in wild-type mice (Figure 2A and B), the enhanced sensitivity in *Phd2*$^{+/-}$ mice was progressively reduced between 2 and 7 d of treatment with PT2385 (Figure 2C and D). The delayed onset of the drug effect in *Phd2*$^{+/-}$ (versus acclimatised wild-type) mice likely reflects the constitutive nature of the genetic intervention, whose long-term consequences may be slow to reverse. Indeed, *Phd2*$^{+/-}$ mice have enlarged carotid bodies which may contribute to their exaggerated hypoxic ventilatory responses (25). Together these results demonstrate that, as well as preventing its development, PT2385 can reverse ventilatory acclimatisation to hypoxia and pseudohypoxia.

Interestingly, in addition to reducing the enhanced ventilatory sensitivity in *Phd2*$^{+/-}$ mice, we noted that PT2385 appeared to reduce ventilatory sensitivity even in their wild-type littermates (filled versus open black circles, Figure 2C and D). Such an effect on baseline (unacclimatised) ventilatory sensitivity was also suggested by a reduction in sensitivity below the baseline in mice exposed to 7 d of hypoxia and treated with PT2385 at a dose of 10 mg kg^{-1} (Figure 1 and Table 1). Therefore, we also performed experiments to assess the effects of PT2385 on baseline ventilatory sensitivity, including the dose and time-dependence of any activity. In these experiments, wild-type male mice were treated with PT2385 or vehicle and their ventilatory sensitivity measured after 1, 5 and 24 h, using the same acute (5 min) gas challenges as described above. Since baseline acute ventilatory responses in unacclimatised mice are small relative to confounding behavioural variations in ventilation when test gases are introduced to the plethysmograph, quantitative data is presented as the average ventilation over the entire period of acute gas exposure (Figure 3B, S5A and S6). Responses are shown in full for selected experiments in Figure 3A. These experiments revealed a clear,

though partial, loss of sensitivity to gas challenge with 10 % oxygen with 3 % carbon dioxide in mice treated with PT2385 at 10 mg kg^{-1} (Figure 3). This reduction in ventilatory sensitivity was similar at all time-points, including 1 h after the first dose of PT2385, and was most clearly manifest as a reduction in tidal volume as opposed to respiratory rate (Figure S5A). Interestingly, these effects were not observed with PT2385 at 3 mg kg^{-1} (Figure S6), suggesting different dose-dependence from actions of PT2385 in acclimatised mice (Figure 1 and S1, Table 1). Of significance, there were no differences in ventilatory sensitivity to carbon dioxide at either dose (Figure 3B and S6), suggesting that PT2385 primarily alters hypoxic, but not hypercapnic, responses. Similar effects on acute hypoxic ventilatory control were observed when wild-type female mice were treated with 3 or 10 mg kg^{-1} (Figure S5B and S7). Together, this data suggests that PT2385, in addition to ablating ventilatory acclimatisation, exerts rapid effects (within 1 h) on acute hypoxic ventilatory control.

PT2385 treatment prevents carotid body cellular and proliferative responses to sustained hypoxia

Along with ventilatory changes, sustained hypoxia induces proliferation of multiple cell types within the carotid body, resulting in hyperplasia of the organ (19, 29). To analyse the effects of PT2385 on this cellular proliferative response, BrdU incorporation was measured in male mice treated with PT2385 or vehicle, and subjected to the same sustained exposure to hypoxia as used in the ventilatory experiments (7 d at 10 % oxygen), or maintained in normal air. In animals given BrdU and maintained for 7 d in normal air, few BrdU-positive cells were observed in carotid bodies from either PT2385- or vehicle-treated mice. Following 7 d at 10 % oxygen, striking incorporation of BrdU across multiple cell types (including Type I and

endothelial cells) in the carotid body (but not in surrounding tissues such as the supracervical ganglion) was observed in vehicle-treated mice (Figure 4 and data not shown). Treatment of the hypoxia-exposed mice with either 3 or 10 mg kg^{-1} PT2385 twice daily resulted in near-total loss of BrdU-positive cells across all cell types (Figure 4 and Figure S8) and prevented the associated increase in carotid body size (Figure 4A). Although the circuitry mediating proliferative responses of the carotid body to hypoxia is not well understood, the HIF transcriptional target gene *Vegfa* has been reported to be induced by hypoxia in Type I cells (19) and may be important in mediating proliferative responses by paracrine signalling to other neighbouring cell populations. Responses of *Vegfa* mRNA to hypoxic exposure were therefore also measured in these animals by in situ hybridisation. The marked induction of *Vegfa* mRNA observed in Type I cells of hypoxic carotid bodies was also greatly reduced by 10, but not 3, mg kg^{-1} PT2385 treatment (Figure 4 and Figure S8). Female mice subjected to the same sustained hypoxia protocol above exhibited high levels of proliferation and *Vegfa* mRNA expression in the carotid body as observed in male mice; these hypoxia-induced changes were likewise prevented by concomitant twice daily 10, and to a lesser extent 3, mg kg^{-1} PT2385 treatment (Figure S9).

In addition to proliferative changes in Type I cells, sustained hypoxia induces HIF-2α-dependent changes to Type I cell ultrastructure as assessed by electron microscopy (19). These hypoxia-induced changes include a reduction in dense core vesicles (DCVs) in Type I cells and an increased frequency of 'eccentric' DCVs with an expanded vesicle and a displaced dense core (19, 30). Strikingly, PT2385 treatment of hypoxic male mice prevented these changes, such that DCVs appeared similar to those observed in mice breathing normal air (Figure 4B), indicating that HIF-2α has a role, directly or indirectly, in the secretory process itself, for example, by altering the expression of gene(s) involved in the regulation of secretion

and/ or DCV content. Together, these data suggest that PT2385 blocks both proliferation and oxygen-dependent vesicular functions of Type I cells of the carotid body, and that both these changes might contribute to reduced ventilatory sensitivity and an inability of PT2385-treated mice to acclimatise to hypoxia.

The S305M mutation in HIF-2α confers resistance to PT2385 without altering HIF-2α protein stability or mRNA expression

The class of HIF-2α antagonists that includes PT2385 binds directly to a pocket within the PAS-B domain of the HIF-2α, but not HIF-1α, protein and allosterically weakens HIF-2α-HIF-1β heterodimer stability (10, 11, 31). To investigate the specificity of this action, the effect of PT2385 on HIF-2α bearing a point mutation located in the HIF-2α PAS-B domain (S305M in the mouse sequence (32)) was tested. This mutation was originally selected based on its location and ability to interfere with the binding of other HIF-2α antagonists acting within the same binding site (10). The mutant methionine residue could in principle block the drug binding pocket locally, or alter the overall conformation and stability of the protein to weaken drug binding. Using proteins expressed and purified in *E. coli* and isothermal titration calorimetry (ITC), we measured the equilibrium dissociation constant (K_d) of PT2385 binding to wild-type mouse HIF-2α PAS-B domain to be 15.4 nM. By comparison, the K_d of PT2385 binding to mouse HIF-2α S305M mutant PAS-B domain was 0.97 μM, indicating a more than 60 fold loss in binding affinity (Figure 5A). These biochemical measurements confirmed that PT2385 binding is substantially reduced in the context of this point mutation. We then investigated whether loss of PT2385 binding was due to binding site occlusion or a loss of overall protein stability caused by the point mutation. Protein thermal shift assays were

applied to determine the melting temperature (T_m) of S305M and wild-type mouse HIF-2α purified proteins. T_m values were similar for wild-type and S305M HIF-2α proteins, in the context of both their isolated PAS-B domains alone and their HIF-2α-HIF-1β heterodimers consisting of their larger bHLH-PAS-A-PAS-B segments (Figure 5B). Closely similar T_m values for wild-type and S305M proteins indicate that the point mutation does not alter the global fold or stability of HIF-2α protein or the stability of its heterodimeric complex with HIF-1β. We infer that the loss of PT2385 binding to the S305M protein is due to the larger methionine (versus serine) side-chain locally occluding the PAS-B pocket where PT2385 physically binds, causing a > 60 fold loss of binding affinity.

Mice engineered to carry this mutation constitutively (herein referred to as *Epas1*$^{S305M/S305M}$ mice) have been described to have broadly unaffected levels of *Hif-2α* mRNA and protein expression in the kidney (33). To test whether this is the case in the carotid body, *Hif-2α* mRNA levels were assessed by in situ hybridisation and quantitative Real-Time PCR in carotid bodies from *Epas1*$^{S305M/S305M}$ mice (Figure 5C). *Hif-2α* mRNA was abundantly expressed in carotid bodies from wild-type mice and levels were similarly high in carotid bodies from *Epas1*$^{S305M/S305M}$ mice (Figure 5C). Taken together, these findings indicate that the S305M mutation confers resistance to PT2385 without altering the expression or conformation of HIF-2α.

PT2385 has no effect on ventilatory or carotid body responses to hypoxia in Epas1$^{S305M/S305M}$ *mice*

To test whether ventilatory sensitivity is altered by PT2385 in *Epas1*$^{S305M/S305M}$ mice, male *Epas1*$^{S305M/S305M}$ mice and wild-type littermate controls were exposed to hypoxia and

administered 10 mg kg^{-1} PT2385, or vehicle, twice daily. As before, ventilatory sensitivity was assessed prior to the start of PT2385 treatment and after exposure to periods of sustained hypoxia of up to 7 d (Figure 6 and Table 2). In striking contrast to wild-type mice, treatment of *Epas1*$^{S305M/S305M}$ mice with PT2385 did not reduce ventilatory sensitivity at any time-point during sustained hypoxia (Figure 6A, B and Table 2). Interestingly, although manifesting clear increases in ventilatory sensitivity after 2 d of hypoxia, untreated *Epas1*$^{S305M/S305M}$ mice did not show further increases as hypoxia was maintained, their ventilatory sensitivity after 7 d exposure to hypoxia being clearly reduced compared to wild-type littermates (7.04 ± 0.47 versus 9.11 ± 0.72 mL min^{-1} g^{-1}, Student's two-tailed *t*-test *P* = 0.032)(Figure 6C and Table 2).

To assess whether *Epas1*$^{S305M/S305M}$ mice are also resistant to PT2385-mediated effects on the cellular and proliferative responses to hypoxia, carotid bodies were examined from the same *Epas1*$^{S305M/S305M}$ mice and compared with the same littermate control mice as were used for the ventilatory measurements described above. High levels of BrdU incorporation were observed in wild-type mice following 7 d at 10 % oxygen and were largely abolished by twice daily treatment with 10 mg kg^{-1} PT2385 (Figure 7). Although there was greater variability in this response, with regional variations in BrdU incorporation, this response (and the accompanying carotid body hyperplasia) was unaffected by PT2385 treatment in *Epas1*$^{S305M/S305M}$ littermate mice (Figure 7). As with earlier experiments (Figure 4), *Vegfa* mRNA was strongly induced in Type I cells of the carotid body by exposure of the wild-type mice to 10 % oxygen for 7 d; this induction of *Vegfa* mRNA was largely ablated by PT2385 (Figure 7). In contrast, PT2385 had little or no effect on hypoxia-induced *Vegfa* mRNA levels in Type I cells in littermate mice of *Epas1*$^{S305M/S305M}$ genotype (Figure 7).

Taken together, these findings indicate that *Epas1*$^{S305M/S305M}$ mice are resistant to the effects of PT2385 on ventilatory sensitivity and cellular changes in the carotid body that are induced by sustained hypoxia, consistent with these actions of PT2385 being on-target to HIF-2α. Unexpectedly, responses to sustained hypoxia were also reduced in untreated *Epas1*$^{S305M/S305M}$ mice, when compared to wild-type littermates.

Discussion

Our findings reveal major effects of the small molecule HIF-2α antagonist PT2385 on hypoxic ventilatory control. Particularly striking were effects on the enhanced ventilatory sensitivity that develops after exposure to a period of sustained hypoxia. This response was essentially ablated at PT2385 doses that are identical to those showing efficacy in studies of patient-derived ccRCC xenografts in the mouse (14). Hypoxic ventilatory sensitivity is considered to be largely mediated by the carotid body, which also responds to sustained hypoxia with changes in gene expression, ultrastructural alterations to dense core vesicles in the secretory Type I cells and a marked multi-lineage cellular proliferation (19, 34). All these responses were abrogated, or greatly reduced, by PT2385. In contrast, such effects were not seen, or were markedly reduced, in mice bearing a mutation in the HIF-2α PAS-B pocket, which was shown to greatly reduce binding of PT2385 to the HIF-2α polypeptide, strongly suggesting that they represent specific on-target effects exerted through an action on HIF-2α.

These findings are of both clinical and biological significance. From the clinical perspective, they establish that PT2385 has a range of effects on the medical physiology of hypoxia in non-neoplastic tissues, which are manifest at the same doses as anti-tumour effects reported in mouse xenograft studies (14). Plasma levels of PT2385 achieved using the recommended phase II dose of 800 mg twice daily (15) were similar or higher than those achieved in the mouse study, suggesting that these effects in the mouse are likely relevant to clinical use of the molecule. Recent work has demonstrated effects of a related molecule PT2399 on hypoxia-stimulated erythropoietin production (12, 33). Our work shows marked effects of PT2385 on hypoxic ventilatory control that are as pronounced or more pronounced than the erythropoietic effects in the context of sustained hypoxia. Taken together, this suggests that

PT2385 is likely to have broad effects on physiological and pathophysiological responses that are mediated by HIF-2α. These might include potentially beneficial effects (such as on neovascularization, pulmonary hypertension or immune activation)(3) or potentially adverse effects such as the associated anaemia that has been reported in clinical trials of PT2385 to date (15, 17). Importantly in this context, the effects on ventilatory control that were observed were highly specific for hypoxia. In unacclimatised mice, we did not observe effects of PT2385 on resting ventilation in normal air or on responses to carbon dioxide. In general, PT2385 was well-tolerated. Despite striking reduction in the enhanced ventilatory sensitivity to hypoxia which is observed in mice acclimatised by exposure to 10 % oxygen, this hypoxic stress (which is equivalent to an altitude of approximately 5500 m above sea level) was also well-tolerated. Consistent with the classical theory on the importance of carbon dioxide in respiratory control, our demonstration of specific effects on responses to hypoxia suggests that PT2385 should not interfere markedly with respiratory control under most circumstances. Nevertheless, the findings suggest that caution will be required in the clinical use of these compounds in some patients, for instance those with chronic pulmonary diseases and reduced ventilatory sensitivity to carbon dioxide, or those at altitude, who may be relying on enhanced sensitivity to hypoxia to maintain stable respiration. Indeed, arterial desaturation was reported in published clinical studies (15, 17), although details of the circumstances surrounding the episodes or the altitudes at which the patients resided were not provided.

The HIF-2α isoform is expressed at unusually high levels in the carotid body (19, 35-37). In keeping with this, several, but not all, genetic studies in the mouse have highlighted the importance of HIF-2α in carotid body responses to hypoxia (19-21, 38). Thus, genetic inactivation of HIF-2α, either generally or specifically, in Type I cells has been reported to

affect both the enhanced ventilatory sensitivity that is observed with exposure to sustained hypoxia and the proliferative responses of the carotid body that are observed in that setting (19, 20). Inactivation of HIF-2α in carotid body Type I cells using Cre-recombinase driven by a TH promoter also leads to severe developmental changes in the carotid body resulting in a non-functional vestigial organ in adult life (21). In contrast, other studies have reported much milder phenotypes, or even enhanced ventilatory sensitivity to hypoxia, in association with heterozygous inactivation of HIF-2α (39, 40). The reasons for these discrepancies among published genetic studies are not known. The current findings provide data, using an orthogonal mode of intervention, corroborating genetic evidence for the importance of HIF-2α in carotid body physiology as well as highlighting the medical implications of its antagonism. Importantly, pharmacological antagonism has also allowed us to assess early time-points following HIF-2α inactivation, revealing the surprisingly rapid onset of the effects on ventilatory control.

PT2385 binds to HIF-2α and has been shown to impair its dimerisation with HIF-1β, thus preventing the formation of the DNA-binding complex and blocking HIF-2 transcriptional activity (12-14, 31). Most of our findings are consistent with this mode of action. We observed reduction in the expression of *Vegfa* mRNA, which is a HIF-2 target gene in the carotid body (19). Most of the effects of PT2385 were also manifest after a delay that was compatible with an effect on transcriptional output. Thus, it appears likely that transcriptional responses mediated by HIF-2 are responsible, directly or indirectly, for the functional, ultrastructural and proliferative responses that take place in the carotid body in response to sustained hypoxia, and that despite very high levels of HIF-2α in that organ (19, 35-37), these responses to hypoxia are very effectively prevented by PT2385. Nevertheless, some of our findings suggest that the role of HIF-2α in the carotid body may be more complex. First, at higher

doses of PT2385, we observed a significant reduction in the baseline hypoxic ventilatory sensitivity in unacclimatised mice, which was manifest within 1 h of exposure to the compound, perhaps representing an action of HIF-2α (or even another PAS domain containing protein) on a process more rapid than transcription. Second, we noted that *Epas1*$^{S305M/S305M}$ mutant mice showed a hypomorphic phenotype with respect to sensitivity to hypoxia, even in the absence of PT2385 and in spite of unaltered dimerisation with HIF-1β. Ventilatory sensitivity in mice is notoriously strain-dependent (41, 42). Nevertheless, this mutant allele was carried in the same strain (33) as the mice used in all other studies (19, 20, 25). We were also careful to focus our comparative studies on mice with and without the S305M mutation that were obtained from the same litter. These studies clearly revealed reduced hypoxic ventilatory sensitivity in *Epas1*$^{S305M/S305M}$ mice exposed to sustained hypoxia, though responses to carbon dioxide were identical to those of wild-type animals and their carotid bodies appeared morphologically normal. Proliferative responses of cells within the carotid body were also more variable and somewhat reduced in *Epas1*$^{S305M/S305M}$ mice. Interestingly, similar findings were recently reported in *Epas1*$^{S305M/S305M}$ mice with respect to erythropoietin production in response to hypoxic stimulation (33). One possibility which has attracted considerable interest, and is raised again by the current findings, is that the PT2385 binding pocket is the target of an endogenous ligand of HIF-2α that normally contributes to the regulation of transcriptional, or even non-transcriptional, actions of HIF-2α (33, 43). Under this hypothesis, it is possible that the hypomorphic phenotype of *Epas1*$^{S305M/S305M}$ mice, with respect to responses to hypoxia, derives from interference with the binding of such a ligand. Resolving whether or not this is the case will require further work. Nevertheless, what is clear from the current work is that molecules targeting HIF-2α in this manner open the way to exploring such possibilities, as well as providing an exciting new realm of clinical investigation

into the potential utility and risks of their use in non-neoplastic, as well as neoplastic, conditions that are associated with the activation of HIF-2.

Methods

Animals

Mice were housed in the Functional Genetics Facility of the Wellcome Trust Centre for Human Genetics (University of Oxford, UK) in individually ventilated cages with food and water provided *ad libitum* and on a 12 h light/ 12 h dark cycle. Male (or, where stated, female) mice aged ~8 weeks old were used in all experiments; all genotypic comparisons were with littermate and sex-matched controls. *Epas1*$^{S305M/S305M}$ mice (as described in (33)), *Phd2*$^{+/-}$ mice (as described in (25)) and wild-type mice were on a C57BL/6 genetic background.

Sustained hypoxic exposure of mice and drug administration

For mouse experiments, PT2385 ((S)-3-((2,2-Difluoro-1-hydroxy-7-(methylsulfonyl)-2,3-dihydro-1 H-inden-4-yl)oxy)-5-fluorobenzonitrile)(MedChemExpress) was suspended in 5 mg mL^{-1} methyl cellulose (Sigma) with 0.5 % Tween 80 (Sigma), to a final concentration of 0.75 mg mL^{-1} or 2.5 mg mL^{-1}, as described in (14). All mice were treated twice daily by oral gavage with 3 or 10 mg kg^{-1} PT2385 (4 mL kg^{-1}), or an equivalent volume of vehicle as control. Mice were given 50 mg kg^{-1} BrdU (Sigma), dissolved in aqueous phosphate buffer pH 7.0 (Fisher Scientific) via i.p. injection immediately prior to exposure to hypoxia or normoxia, followed by supplementation of drinking water with BrdU (1 mg mL^{-1} and 1 % sucrose) for the 7 d experimental period. For sustained exposures to hypoxia, mice were placed into a normobaric altitude chamber and acclimatised to decreasing oxygen levels over 24 h, and then maintained at 10 % oxygen for 7 d with controlled temperature, humidity and carbon dioxide levels and free access to food and water (25). Mice were briefly removed from the normobaric altitude chamber in order to perform plethysmography measurements (30 min in normal air,

then 30 min in unsealed plethysmographs followed by 3 cycles of: 5 mins medical air/ 5 min acute gas challenge/ 5 min medical air with 15 min in unsealed plethysmographs between the cycles) and/ or oral treatment with PT2385 or vehicle. Normoxic littermate controls were maintained under normal housing conditions. All mice were weighed at the start of the procedure and monitored daily for general condition and changes in body weight. No significant differences in body weight were noted with PT2385 treatment and/ or in *Epas1*$^{S305M/S305M}$ mice.

Plethysmography

Tidal volume and respiratory rate were measured in awake, unrestrained mice using whole-body plethysmographs (600 mL; Model PLY4211; Buxco)(25). Minute ventilation was calculated from tidal volume and respiratory rate. Ventilatory parameters were derived using FinePointe software (Buxco) and normalised to body weight as measured immediately prior to plethysmography. Premixed gas was delivered to each chamber as described previously (25). The acute gas challenge consisted of 10 % oxygen, balance nitrogen; 10 % oxygen, 3 % carbon dioxide, balance nitrogen; or 21 % oxygen, 3 % carbon dioxide, balance nitrogen. The acute ventilatory response (AVR) to each stimulus was defined as the difference between minute ventilation during the 1 min prior to the onset of acute gas challenge and the first 1 min of stable acute gas exposure (following a 30 s delay period after switching the gas mixtures).

For unacclimatised measurements, mice were treated with the first dose of PT2385 (or vehicle) and ventilation was measured by plethysmography 1 and 5 h following this dose,

after which the second dose of PT2385 (or vehicle) was administered. The following day, ventilation was measured 24 h following the first dose.

For measurements of ventilatory sensitivity in animals exposed to sustained hypoxia, mice were given PT2385 (or vehicle) twice daily for 24 h then placed into the normobaric altitude chamber and twice daily PT2385 (or vehicle) treatment continued. Plethysmography measurements were made following 2, 5 and 7 d of sustained hypoxia in the morning, prior to the first daily dose of PT2385.

Blood measurements

Blood was obtained from the inferior vena cava of mice using heparinised capillary tubes after terminal anaesthesia and haematocrits measured using a haematocrit centrifuge (mode C-MH30; Unico).

Tissue preparation

Mice were killed by overdose of isoflurane (Piramal Critical Care)(in the altitude chamber for the hypoxic mice) and exsanguination. This was followed by dissection of tissues, which were then immersion-fixed in 4 % paraformaldehyde/ PBS (Sigma) overnight. Tissues were then transferred to 70 % ethanol and progressively dehydrated in an ascending ethanol series prior to paraffin-embedding. Paraffin-embedded tissues were sectioned to 4 µm using an RM135 microtome (Leica Biosystems).

Immunohistochemistry and in situ hybridisation

Paraffin-embedded sections were immunostained with anti-TH (dilution 1:5000; NB300-109; Novus Biologicals) or with an anti-BrdU antibody (dilution 1:10; #551321; Becton Dickinson Biosciences), as described previously (25). *Vegfa* and *Hif-2α* mRNA transcripts were detected via in situ hybridisation on sections from paraffin-embedded tissues using the manual RNAscope 2.5 HD BROWN assay (Advanced Cell Diagnostics). Samples were imaged using a DM 1000 LED microscope (Leica Biosystems). Stereological estimation of cell number, cell density and carotid body volume was performed using ImageJ (NIH) on every fourth paraffin section (25). In situ hybridisation probe signal was quantified using trainable Weka segmentation in FIJI ImageJ software, according to the manufacturer's instructions.

Electron microscopy

Tissue samples for electron microscopy (EM) were harvested immediately after terminal anaesthesia and immersion-fixed in 4 % formaldehyde and 2.5 % glutaraldehyde in 0.1 M phosphate buffer pH 7.4 for 1 h at room temperature. Tissue was post-fixed in 2 % aqueous osmium tetroxide for 1 h at 4 °C. Tissue was rinsed in water, stained with 2 % aqueous uranyl acetate overnight at 4 °C, dehydrated in an ascending ethanol series, infiltrated with epon resin mixed with propylene oxide and embedded in 100 % epon resin. To determine the location of the carotid body, the polymerised sample was imaged using microCT (Zeiss Xradia 510 Versa) with a Zeiss filter LE2 and 4 x objective lens. To confirm the presence of the carotid body by light microscopy, semi-thin sections were produced and stained using toluidine blue, as described previously (44). Ultrathin sections were produced and stained, as described

previously (45). EM imaging was performed using a Tecnai G2 Spirit BioTWIN transmission EM (ThermoFisher Scientific) equipped with OneView CMOS camera (Gatan).

Quantitative Real-Time PCR

Carotid artery bifurcations were dissected from 5 littermate pairs of wild-type and *Epas1*$^{S305M/S305M}$ mice maintained in 10 % oxygen for 7 d and transferred into ice-cold PBS. Carotid bodies were sub-dissected and stored in RNA*later* (Qiagen) on ice. Carotid bodies from all animals per genotype were then pooled and RNA was isolated and cDNA prepared as described in (35). *Hif-2α* mRNA was quantified in triplicate in a duplex quantitative Real-Time PCR reaction using the TaqMan Fast Advanced Master Mix and the *Hif-2α* (*Epas1*) FAM and *Actb* VIC TaqMan Gene expression Assays (Mm00438712_m1 and Mm01205647_g1, ThermoFisher Scientific). The reaction was carried out in the StepOnePlus Real-Time PCR System (Applied Biosystems). ΔC_T was defined as the difference between the *Epas1* C_T and the *Actb* C_T. $-\Delta\Delta C_T$ values were calculated for each replicate as – (*Epas1*$^{S305M/S305M}$ ΔC_T - wild-type ΔC_T)(46). Fold change in the *Epas1* mRNA expression in each genotype group was expressed as $2^{-\Delta\Delta CT}$.

Plasmid construction and site-directed mutagenesis

Mouse HIF-2α PAS-B domain (241-361) was cloned into pSJ2 vector, as previously described (31). Mutation of S305M was introduced using the QuikChange II XL site-directed mutagenesis kit (Agilent).

Protein expression and purification

Wild-type mouse HIF-2α PAS-B domain and the S305M mutation were both expressed and purified, as previously described (31). HIF-2α-HIF-1β heterodimers (wild-type and with the S305M mutation in the HIF-2α subunit) consisting of bHLH-PAS-A-PAS-B domains were expressed and purified using the co-expression constructs and procedures previously published (31).

Isothermal titration calorimetry

PT2385 (Abcam) was initially dissolved in DMSO and then diluted 1:1000 in buffer with 20 mM Tris pH 8.0 and 150 mM NaCl. Temperatures were measured on a Nano ITC system (TA instruments), with HIF-2α PAS-B domains in 20 mM Tris pH 8.0, 150 mM NaCl and 0.1 % DMSO at 20 °C. 30 aliquots of 7.98 µL of 200 µM HIF-2α PAS-B domain, or the S305M mutation, were injected into 40 µM PT2385. Stoichiometry, binding constant and change in enthalpy of interaction were calculated using the ITCRun and NanoAnalyze software (TA instruments).

Protein thermal shift

Experiments were carried out on a StepOnePlus Real-Time PCR System (Applied Biosystems) using 2 µM of each protein construct in buffer containing 20 mM Tris pH 8.0 and 150 mM NaCl, as previously described (31). Data were analysed using the DMAN v5.2 (47) to calculate ΔT_m.

Statistical analysis

Data are shown as the mean ± SEM, unless stated otherwise. Details of the statistical tests used are included in the respective figure legends. $P < 0.05$ was considered statistically significant throughout and *P* values corrected for multiple comparisons as indicated. All statistical analyses were performed using GraphPad Prism version 8.2.0.

Study approval

The animal studies were performed under the Home Office animal work project license (PPL P38BE32DE), in accordance with protocols approved by both the Ethics Committee of the University of Oxford and the Home Office under the Animals (Scientific Procedures) Act 1986, United Kingdom.

Author contributions

Experiments were designed by TB and PJR. Data were predominantly collected and analysed by XC, MPB, JWF, MZ, ALB, LMC, FR, TB and PJR with contributions from other authors. The manuscript was written by TB and PJR with input from XC, MPB, JWF, PAR, EJH, FR and reviewed by all authors. Figures were prepared, and statistical analyses were performed, by MPB with input from other authors. Ordering of joint first authors is based on the length of time spent on the project. Joint senior authors TB and PJR conceived the study and managed the project throughout.

Acknowledgements

Funding for the work was received from the Wellcome Trust (106241/Z/14/Z); the Oxford Branch of the Ludwig Institute for Cancer Research and the Paradifference Foundation. This work was also supported by the Francis Crick Institute, which receives its core funding from Cancer Research UK (FC001501); the UK Medical Research Council (FC001501); and the Wellcome Trust (FC001501). JDCCL and LE were sponsored by a FAPESP fellowship (2018/20083-1) and a fellowship from Boehringer Ingelheim Fonds, respectively.

References

1. Keith B, Johnson RS, and Simon MC. HIF1alpha and HIF2alpha: sibling rivalry in hypoxic tumour growth and progression. *Nat Rev Cancer.* 2011;12(1):9-22.
2. Ratcliffe PJ. Oxygen sensing and hypoxia signalling pathways in animals: the implications of physiology for cancer. *J Physiol.* 2013;591(8):2027-42.
3. Semenza GL. Hypoxia-inducible factors in physiology and medicine. *Cell.* 2012;148(3):399-408.
4. Fraisl P, Aragones J, and Carmeliet P. Inhibition of oxygen sensors as a therapeutic strategy for ischaemic and inflammatory disease. *Nat Rev Drug Discov.* 2009;8(2):139-52.
5. Zhang H, Qian DZ, Tan YS, Lee K, Gao P, Ren YR, et al. Digoxin and other cardiac glycosides inhibit HIF-1alpha synthesis and block tumor growth. *Proc Natl Acad Sci U S A.* 2008;105(50):19579-86.
6. Kaelin WG, Jr. The VHL Tumor Suppressor Gene: Insights into Oxygen Sensing and Cancer. *Trans Am Clin Climatol Assoc.* 2017;128:298-307.
7. Kaelin WG, Jr. The von Hippel-Lindau tumour suppressor protein: O2 sensing and cancer. *Nat Rev Cancer.* 2008;8(11):865-73.
8. Kondo K, Kim WY, Lechpammer M, and Kaelin WG, Jr. Inhibition of HIF2alpha is sufficient to suppress pVHL-defective tumor growth. *PLoS Biol.* 2003;1(3):E83.
9. Raval RR, Lau KW, Tran MG, Sowter HM, Mandriota SJ, Li JL, et al. Contrasting properties of hypoxia-inducible factor 1 (HIF-1) and HIF-2 in von Hippel-Lindau-associated renal cell carcinoma. *Mol Cell Biol.* 2005;25(13):5675-86.

10. Rogers JL, Bayeh L, Scheuermann TH, Longgood J, Key J, Naidoo J, et al. Development of inhibitors of the PAS-B domain of the HIF-2alpha transcription factor. *J Med Chem.* 2013;56(4):1739-47.

11. Scheuermann TH, Li Q, Ma HW, Key J, Zhang L, Chen R, et al. Allosteric inhibition of hypoxia inducible factor-2 with small molecules. *Nat Chem Biol.* 2013;9(4):271-6.

12. Chen W, Hill H, Christie A, Kim MS, Holloman E, Pavia-Jimenez A, et al. Targeting renal cell carcinoma with a HIF-2 antagonist. *Nature.* 2016;539(7627):112-7.

13. Cho H, Du X, Rizzi JP, Liberzon E, Chakraborty AA, Gao W, et al. On-target efficacy of a HIF-2alpha antagonist in preclinical kidney cancer models. *Nature.* 2016;539(7627):107-11.

14. Wallace EM, Rizzi JP, Han G, Wehn PM, Cao Z, Du X, et al. A Small-Molecule Antagonist of HIF2alpha Is Efficacious in Preclinical Models of Renal Cell Carcinoma. *Cancer Res.* 2016;76(18):5491-500.

15. Courtney KD, Infante JR, Lam ET, Figlin RA, Rini BI, Brugarolas J, et al. Phase I Dose-Escalation Trial of PT2385, a First-in-Class Hypoxia-Inducible Factor-2alpha Antagonist in Patients With Previously Treated Advanced Clear Cell Renal Cell Carcinoma. *J Clin Oncol.* 2018;36(9):867-74.

16. Papadopoulos KP, Jonasch E, Zojwalla NJ, Wang K, and Bauer TM. A first-in-human phase 1 dose-escalation trial of the oral HIF-2a inhibitor PT2977 in patients with advanced solid tumors. *https://doiorg/101200/JCO20183615_suppl2508.* 2018.

17. Strowd RE, Ellingson BM, Wen PY, Ahluwalia MS, Piotrowski AF, Desai AS, et al. Safety and activity of a first-in-class oral HIF2-alpha inhibitor, PT2385, in patients with first recurrent glioblastoma (GBM). *https://doiorg/101200/JCO20193715_suppl2027.* 2019.

18. Jonasch E, Park EK, Thamake S, Hirmand M, Linehan WM, and Srinivasan R. An open-label phase II study to evaluate PT2977 for the treatment of von Hippel-Lindau disease-associated renal cell carcinoma. *https://doiorg/101200/JCO2019377_supplTPS680.* 2019.

19. Fielding JW, Hodson EJ, Cheng X, Ferguson DJP, Eckardt L, Adam J, et al. PHD2 inactivation in Type I cells drives HIF-2alpha-dependent multilineage hyperplasia and the formation of paraganglioma-like carotid bodies. *J Physiol.* 2018;596(18):4393-412.

20. Hodson EJ, Nicholls LG, Turner PJ, Llyr R, Fielding JW, Douglas G, et al. Regulation of ventilatory sensitivity and carotid body proliferation in hypoxia by the PHD2/HIF-2 pathway. *J Physiol.* 2016;594(5):1179-95.

21. Macias D, Cowburn AS, Torres-Torrelo H, Ortega-Saenz P, Lopez-Barneo J, and Johnson RS. HIF-2alpha is essential for carotid body development and function. *Elife.* 2018;7:e34681.

22. Robbins PA. Role of the peripheral chemoreflex in the early stages of ventilatory acclimatization to altitude. *Respir Physiol Neurobiol.* 2007;158(2-3):237-42.

23. Beall CM, Cavalleri GL, Deng L, Elston RC, Gao Y, Knight J, et al. Natural selection on EPAS1 (HIF2alpha) associated with low hemoglobin concentration in Tibetan highlanders. *Proc Natl Acad Sci U S A.* 2010;107(25):11459-64.

24. Cowburn AS, Crosby A, Macias D, Branco C, Colaco RD, Southwood M, et al. HIF2alpha-arginase axis is essential for the development of pulmonary hypertension. *Proc Natl Acad Sci U S A.* 2016;113(31):8801-6.

25. Bishop T, Talbot NP, Turner PJ, Nicholls LG, Pascual A, Hodson EJ, et al. Carotid body hyperplasia and enhanced ventilatory responses to hypoxia in mice with heterozygous deficiency of PHD2. *J Physiol.* 2013;591(14):3565-77.

26. Fatemian M, and Robbins PA. Human ventilatory response to CO2 after 8 h of isocapnic or poikilocapnic hypoxia. *J Appl Physiol (1985).* 1998;85(5):1922-8.

27. Appelhoff RJ, Tian YM, Raval RR, Turley H, Harris AL, Pugh CW, et al. Differential function of the prolyl hydroxylases PHD1, PHD2, and PHD3 in the regulation of hypoxia-inducible factor. *J Biol Chem.* 2004;279(37):38458-65.

28. Berra E, Benizri E, Ginouves A, Volmat V, Roux D, and Pouyssegur J. HIF prolyl-hydroxylase 2 is the key oxygen sensor setting low steady-state levels of HIF-1alpha in normoxia. *EMBO J.* 2003;22(16):4082-90.

29. Pardal R, Ortega-Sáenz P, Durán R, and J. L-B. Glia-like stem cells sustain physiologic neurogenesis in the adult mammalian carotid body. *Cell.* 2007;131(2):364-77.

30. Edwards C, Heath D, and Harris P. Ultrastructure of the carotid body in high-altitude guinea-pigs. *J Pathol.* 1972;107(2):131-6.

31. Wu D, Su X, Lu J, Li S, Hood BL, Vasile S, et al. Bidirectional modulation of HIF-2 activity through chemical ligands. *Nat Chem Biol.* 2019;15(4):367-76.

32. Tian H, McKnight SL, and Russell DW. Endothelial PAS domain protein 1 (EPAS1), a transcription factor selectively expressed in endothelial cells. *Genes Dev.* 1997;11(1):72-82.

33. Feng Z, Zou X, Chen Y, Wang H, Duan Y, and Bruick RK. Modulation of HIF-2alpha PAS-B domain contributes to physiological responses. *Proc Natl Acad Sci U S A.* 2018;115(52):13240-45.

34. Kumar P, and Prabhakar NR. Peripheral chemoreceptors: function and plasticity of the carotid body. *Compr Physiol.* 2012;2(1):141-219.

35. Gao L, Bonilla-Henao V, Garcia-Flores P, Arias-Mayenco I, Ortega-Saenz P, and Lopez-Barneo J. Gene expression analyses reveal metabolic specifications in acute O2 -sensing chemoreceptor cells. *J Physiol.* 2017;595(18):6091-120.

36. Tian H, Hammer RE, Matsumoto AM, Russell DW, and McKnight SL. The hypoxia-responsive transcription factor EPAS1 is essential for catecholamine homeostasis and protection against heart failure during embryonic development. *Genes Dev.* 1998;12(21):3320-4.

37. Zhou T, Chien MS, Kaleem S, and Matsunami H. Single cell transcriptome analysis of mouse carotid body glomus cells. *J Physiol.* 2016;594(15):4225-51.

38. Macias D, Fernandez-Aguera MC, Bonilla-Henao V, and Lopez-Barneo J. Deletion of the von Hippel-Lindau gene causes sympathoadrenal cell death and impairs chemoreceptor-mediated adaptation to hypoxia. *EMBO Mol Med.* 2014;6(12):1577-92.

39. Peng YJ, Nanduri J, Khan SA, Yuan G, Wang N, Kinsman B, et al. Hypoxia-inducible factor 2alpha (HIF-2alpha) heterozygous-null mice exhibit exaggerated carotid body sensitivity to hypoxia, breathing instability, and hypertension. *Proc Natl Acad Sci U S A.* 2011;108(7):3065-70.

40. Yuan G, Peng YJ, Reddy VD, Makarenko VV, Nanduri J, Khan SA, et al. Mutual antagonism between hypoxia-inducible factors 1alpha and 2alpha regulates oxygen sensing and cardio-respiratory homeostasis. *Proc Natl Acad Sci U S A.* 2013;110(19):E1788-96.

41. Han F, Subramanian S, Dick TE, Dreshaj IA, and Strohl KP. Ventilatory behavior after hypoxia in C57BL/6J and A/J mice. *J Appl Physiol (1985).* 2001;91(5):1962-70.

42. Han F, Subramanian S, Price ER, Nadeau J, and Strohl KP. Periodic breathing in the mouse. *J Appl Physiol (1985).* 2002;92(3):1133-40.

43. Scheuermann TH, Tomchick DR, Machius M, Guo Y, Bruick RK, and Gardner KH. Artificial ligand binding within the HIF2alpha PAS-B domain of the HIF2 transcription factor. *Proc Natl Acad Sci U S A.* 2009;106(2):450-5.

44. Graham L, and Orenstein JM. Processing tissue and cells for transmission electron microscopy in diagnostic pathology and research. *Nat Protoc.* 2007;2(10):2439-50.

45. Kume K, Cantwell H, Burrell A, and Nurse P. Nuclear membrane protein Lem2 regulates nuclear size through membrane flow. *Nat Commun.* 2019;10(1):1871.

46. Livak KJ, and Schmittgen TD. Analysis of relative gene expression data using real-time quantitative PCR and the 2(-Delta Delta C(T)) Method. *Methods.* 2001;25(4):402-8.

47. Wang CK, Weeratunga SK, Pacheco CM, and Hofmann A. DMAN: a Java tool for analysis of multi-well differential scanning fluorimetry experiments. *Bioinformatics.* 2012;28(3):439-40.

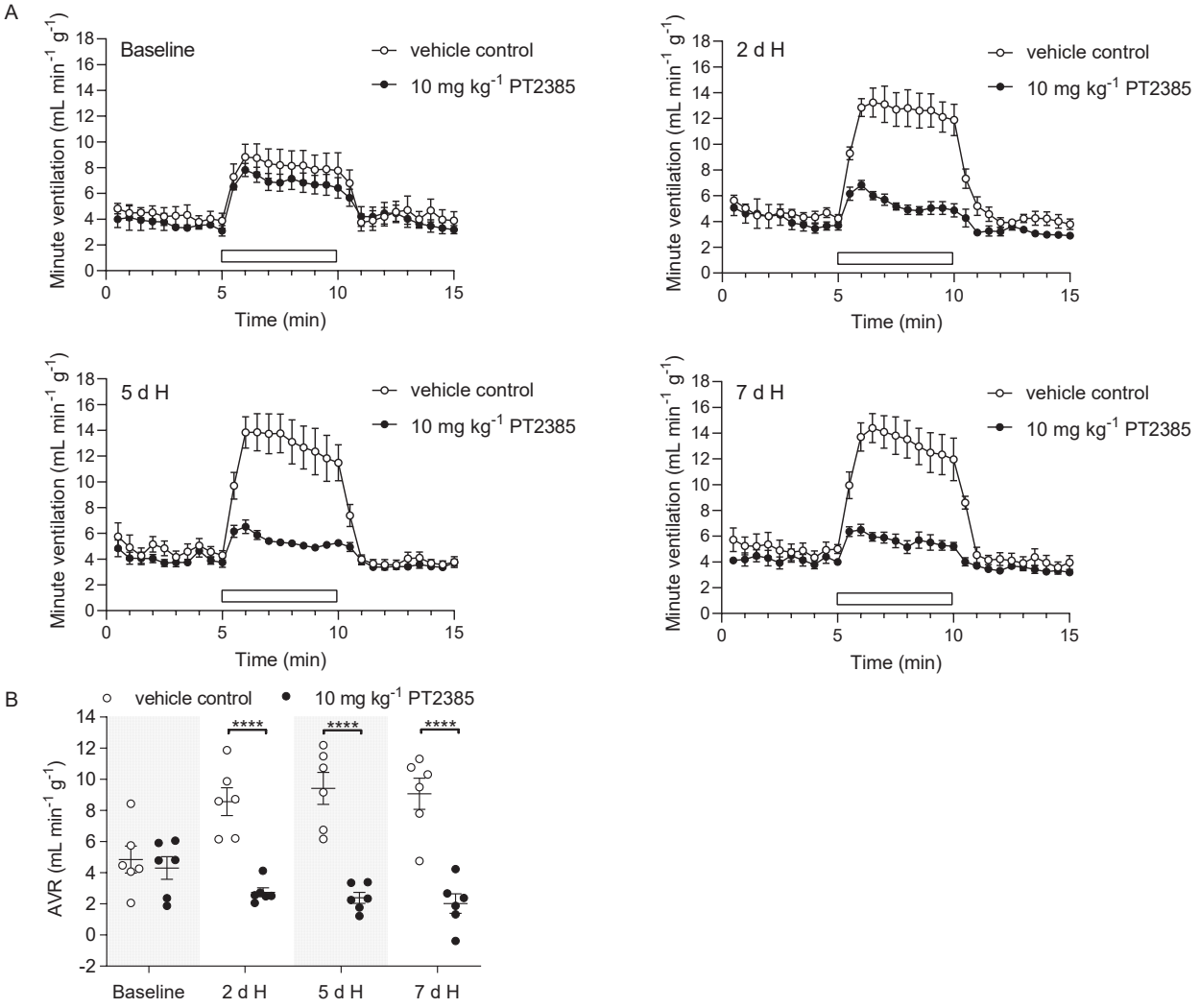

Figure 1. PT2385 ablates ventilatory acclimatisation to hypoxia in wild-type male mice.

(**A**) Graphs show changes in minute ventilation in response to an acute (5 min) challenge with 10 % O_2/ 3 % CO_2 (open bars) in male mice before (Baseline) and following twice daily treatment with 10 mg kg^{-1} PT2385 (or vehicle), beginning 24 h before 7 d exposure to hypoxia (H, 10 % oxygen) and continuing throughout (to a total of 8 d treatment)(n = 6). (**B**) Graph shows acute ventilatory responses (AVRs) to challenges with 10 % O_2/ 3 % CO_2, quantified from the minute ventilation shown in (**A**). Data were analysed by a two-way repeated measures ANOVA with Baseline recordings removed from statistical analysis (P values shown in Table 1), followed by Holm-Sidak's multiple comparisons two-tailed test for individual time-point comparisons, for which the significance is reported in the graph, **** $P < 0.0001$.

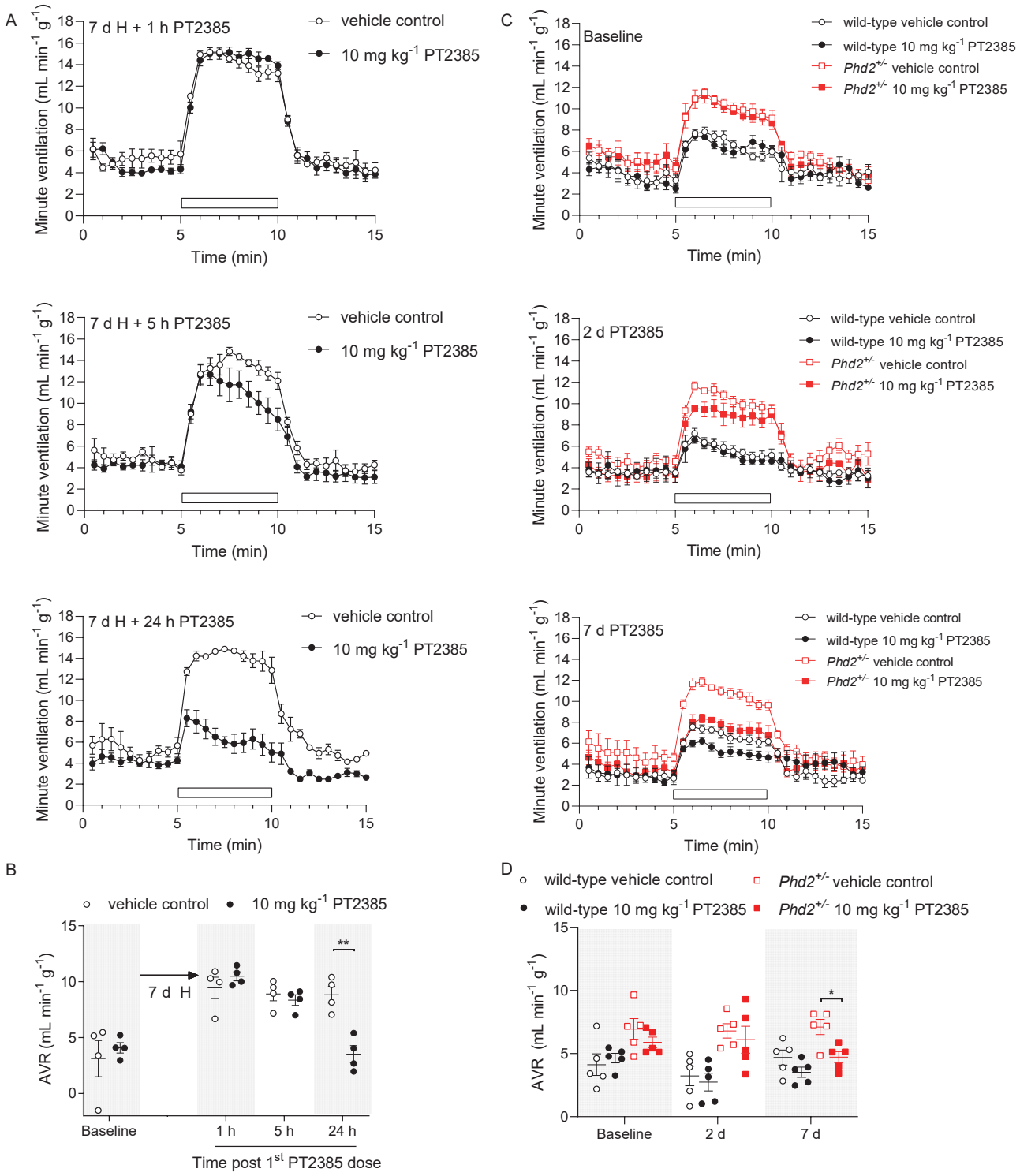

Figure 2. Reversal of enhanced ventilatory sensitivity in acclimatised wild-type and *Phd2*$^{+/-}$ male mice by PT2385.

Graphs illustrate changes in minute ventilation in response to an acute challenge with 10 % O_2/ 3 % CO_2 (open bars) before (Baseline) and at the indicated times after the onset of twice daily treatment with 10 mg kg^{-1} PT2385. (**A**) Male mice were pre-exposed to 7 d hypoxia (H, 10 % oxygen) then treated with PT2385 (or vehicle) in continuing hypoxia (n = 4). (**C**) *Phd2*$^{+/-}$ or littermate wild-type male mice were treated with PT2385 (or vehicle) and maintained in normal air (n = 5). (**B, D**) Summary of acute ventilatory responses (AVRs) calculated from data shown in (**A**, **C**) and from measurements taken before the start of the experiment in (**A**)(Baseline). Data from (**A, C**) were analysed by Holm-Sidak's multiple comparisons two-tailed tests (for all time-points within each genotype for **C**), for which significance is reported in the graphs, * P < 0.05, ** P < 0.01.

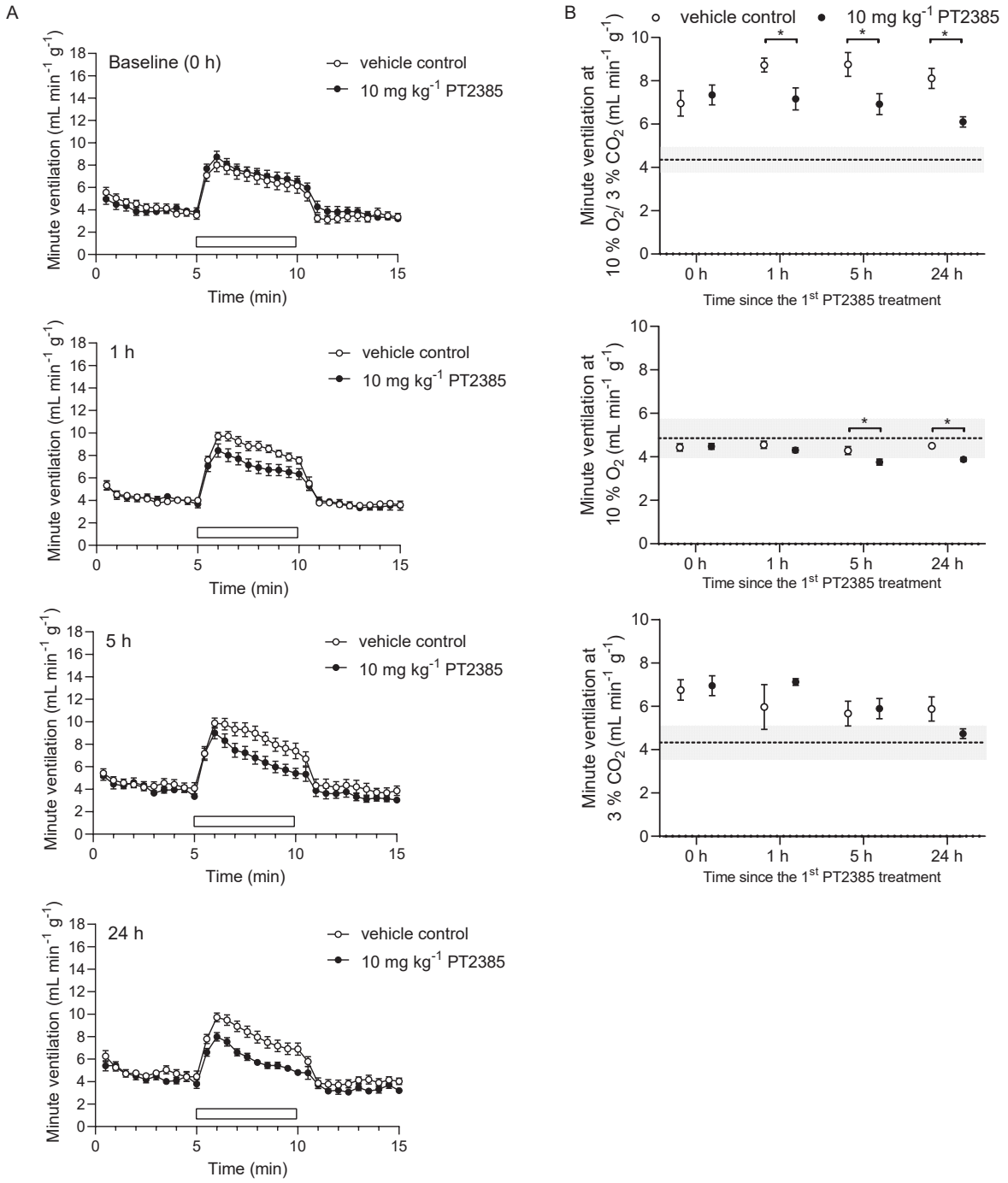

Figure 3. Rapid reduction in ventilatory sensitivity to hypoxia in unacclimatised PT2385-treated male mice.

(**A**) Graphs show changes in minute ventilation in response to an acute (5 min) challenge with 10 % O_2/ 3 % CO_2 (open bars). (**B**) Graphs show average minute ventilation during 5 min challenges with 10 % O_2/ 3 % CO_2 (upper panel), 10 % O_2 (middle panel) or 3 % CO_2 (lower panel). Measurements for (**A, B**) were made before (Baseline, 0 h) and 1, 5 and 24 h after the first 10 mg kg^{-1} PT2385 (or vehicle) dose (n = 15, except for 3 % CO_2 for 1 h where n = 3); second dose of PT2385 was given immediately after the 5 h measurements. Data were analysed by Holm-Sidak's multiple comparisons two-tailed tests, for which the significance is reported in the graphs, * $P < 0.05$. Dotted lines show the average resting minute ventilation in air prior to the acute gas challenge, across all time-points and treatment groups, ± SEM (shaded area).

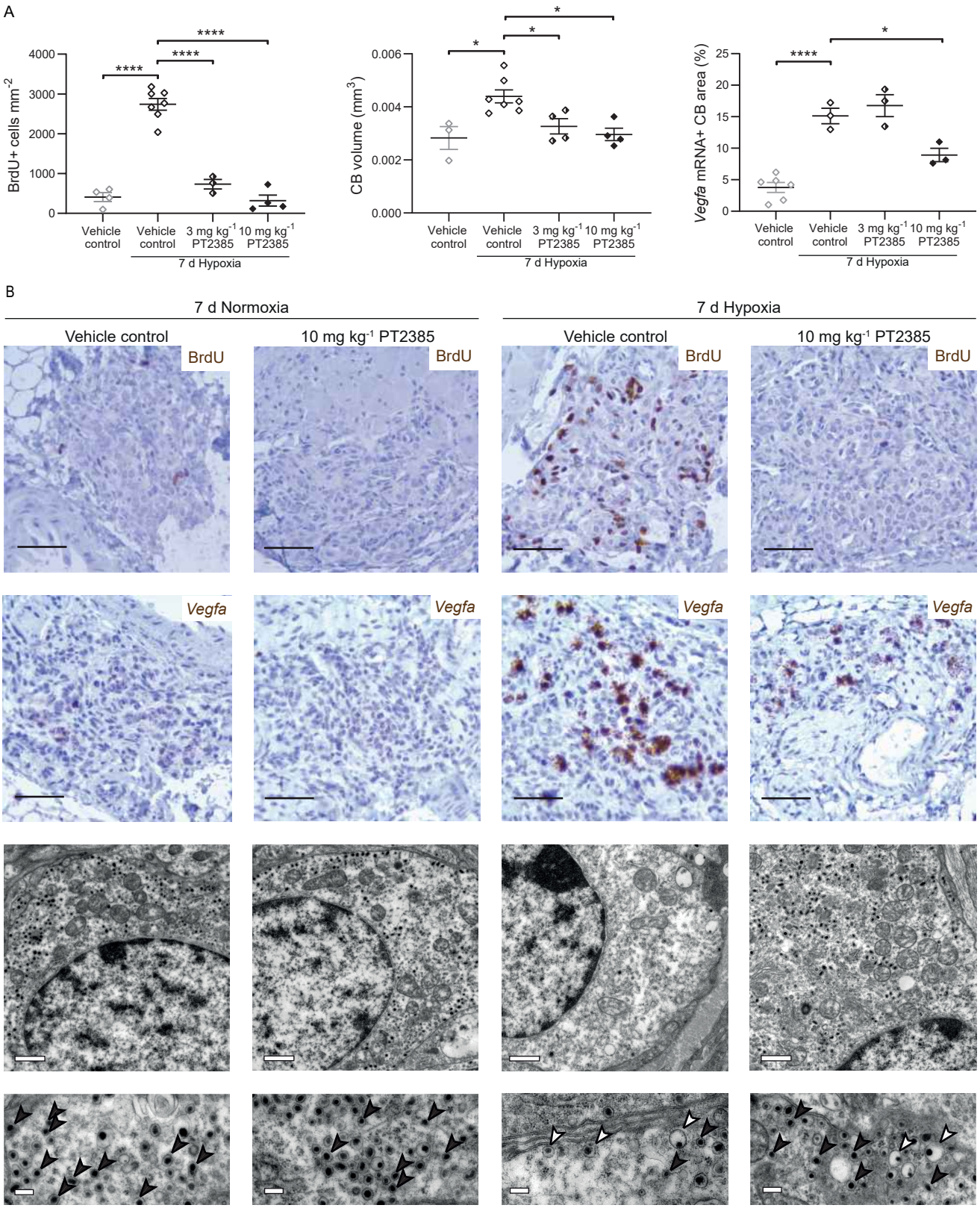

Figure 4. Effects of PT2385 on cellular responses to hypoxia in the carotid body.

(**A**) Morphometry and (**B**) representative images of carotid bodies (CBs) from wild-type male mice exposed to 7 d hypoxia (10 % oxygen), or normoxia, and treated twice daily with 3 or 10 mg kg^{-1} PT2385 (or vehicle), beginning 24 h before and continuing throughout 7 d hypoxia (10 % oxygen) or normoxia (to a total of 8 d treatment). (**A**) Quantification of BrdU+ cells per mm^2 (left panel), CB volumes (middle panel) and *Vegfa* mRNA+ CB area (right panel). Data were analysed by one-way ANOVAs followed by Holm-Sidak's multiple comparisons two-tailed tests, for which significance is reported in the graphs, * $P < 0.05$, **** $P < 0.0001$. (**B**) Immunostaining for BrdU; *Vegfa* mRNA in situ hybridisation; representative electron micrographs showing the dense core vesicles in Type I cells of the CB (note that changes induced by hypoxia are not observed in mice treated with PT2385; compare third and fourth columns)(n = 2). Scale bars represent 50 µm in the top two panels, 1 µm in the top electron micrograph panels and 200 nm in the bottom electron micrograph panels. Filled arrowheads show typical dense core vesicles (DCVs), whilst open arrowheads show 'eccentric' DCVs. Images of CBs of mice treated with 3 mg kg^{-1} PT2385 are shown in Figure S8.

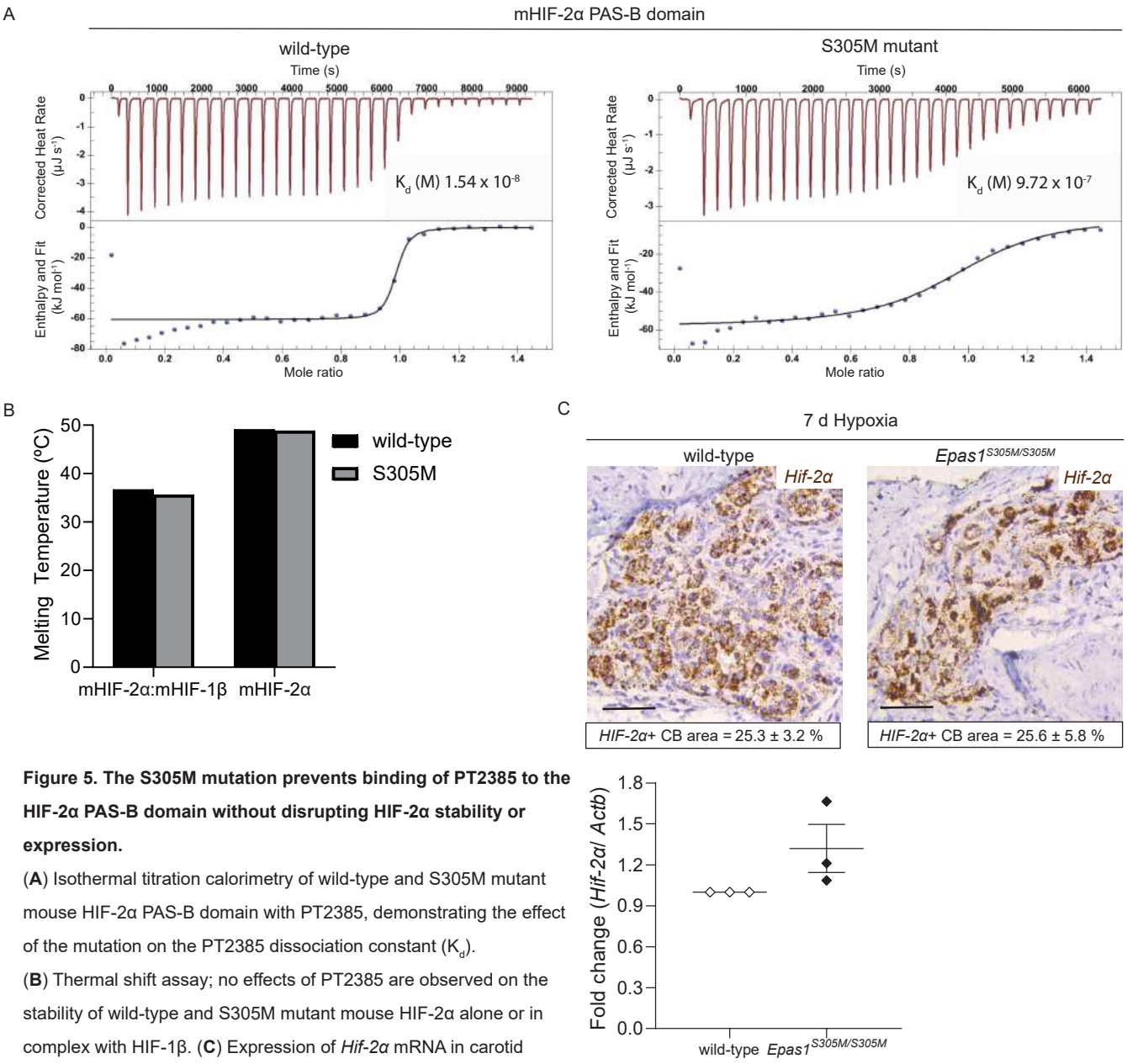

Figure 5. The S305M mutation prevents binding of PT2385 to the HIF-2α PAS-B domain without disrupting HIF-2α stability or expression.

(**A**) Isothermal titration calorimetry of wild-type and S305M mutant mouse HIF-2α PAS-B domain with PT2385, demonstrating the effect of the mutation on the PT2385 dissociation constant (K_d).

(**B**) Thermal shift assay; no effects of PT2385 are observed on the stability of wild-type and S305M mutant mouse HIF-2α alone or in complex with HIF-1β. (**C**) Expression of *Hif-2α* mRNA in carotid bodies (CBs) of wild-type and *Epas1*$^{S305M/S305M}$ mice exposed to 7 d hypoxia (10 % oxygen), as assessed by in situ hybridisation (top panels; scale bars represent 50 μm; quantified *Hif-2α* mRNA+ CB area depicted in boxes below the relevant panel, *n* = 4; data analysed by a two-tailed *t*-test, *P* > 0.05) or quantitative Real-Time PCR (bottom graph). Values are the mean fold change of *Hif-2α* mRNA relative to *Actb* mRNA, from three experiments on CBs pooled from five animals per genotype in each; data analysed by a two-tailed *t*-test, *P* > 0.05.

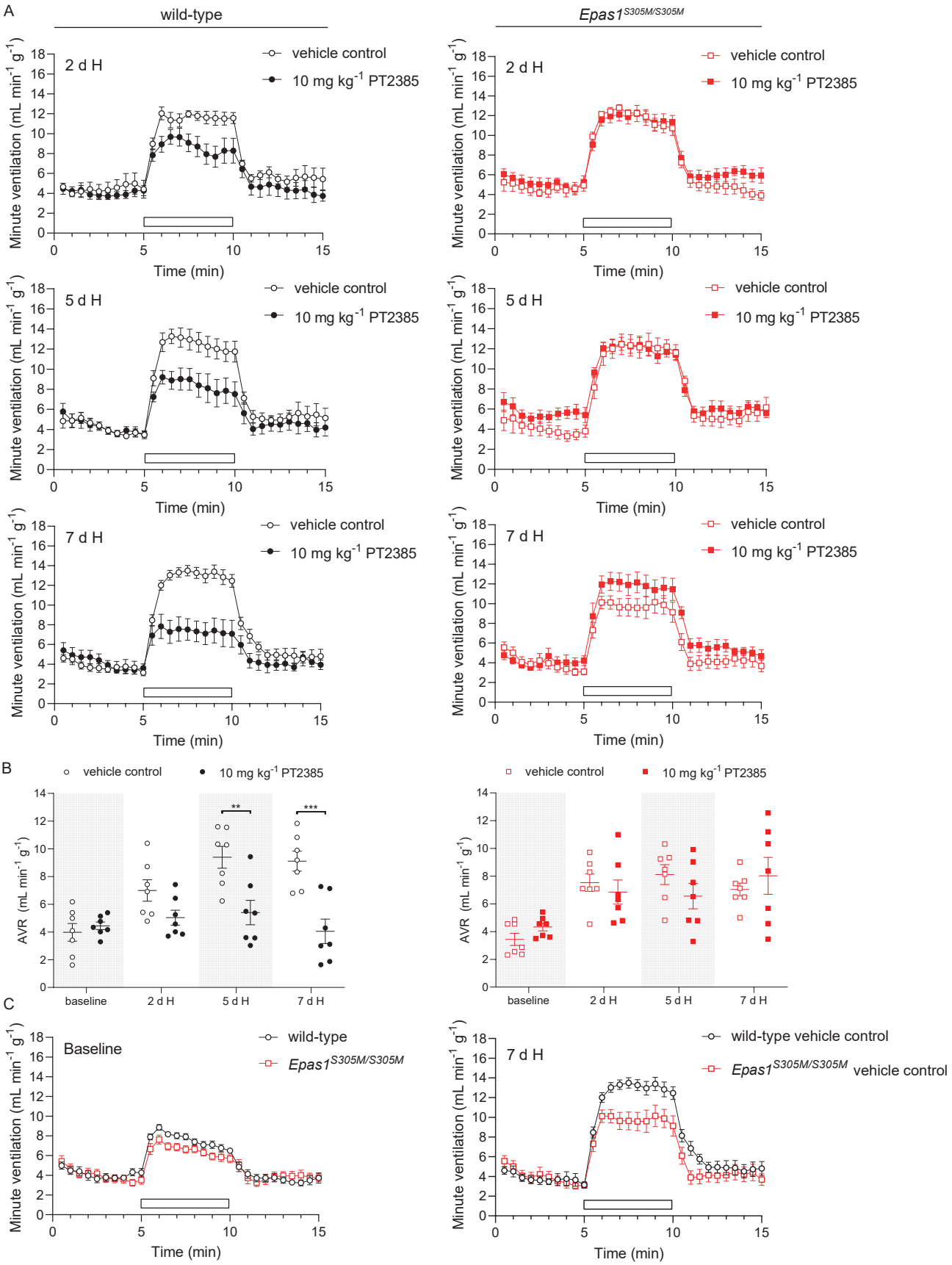

Figure 6. *Epas1*$^{S305M/S305M}$ male mice are resistant to PT2385 effects on enhanced ventilatory sensitivity to hypoxia.

Graphs show minute ventilation in response to an acute (5 min) challenge with 10 % O_2/ 3 % CO_2 (open bars) before (Baseline) and after the indicated exposure to 7 d hypoxia (H, 10 % oxygen). (**A**) Comparison of wild-type and *Epas1*$^{S305M/S305M}$ male mice treated twice daily with 10 mg kg^{-1} PT2385 (or vehicle), beginning 24 h before 7 d exposure to hypoxia and continuing throughout (to a total of 8 d treatment)(*n* = 7). (**B**) Graphs show acute ventilatory responses (AVRs) to challenges with 10 % O_2/ 3 % CO_2, quantified from the minute ventilation in (**A**). Data from each genotype were analysed by a two-way repeated measures ANOVA, with Baseline recordings removed from statistical analyses (*P* values in Table 2), followed by Holm-Sidak's multiple comparisons two-tailed tests for individual time-point comparisons, for which significance is reported in the graphs, ** $P < 0.01$, *** $P < 0.001$. (**C**) Comparison of ventilatory sensitivity in vehicle-treated wild-type and *Epas1*$^{S305M/S305M}$ male mice before (Baseline) and after 7 d exposure to hypoxia. For Baseline comparison, measurements were pooled from all treatment groups per genotype (*n* = 14). Data at 7 d is replotted from (**A**), to provide direct comparison (*n* = 7).

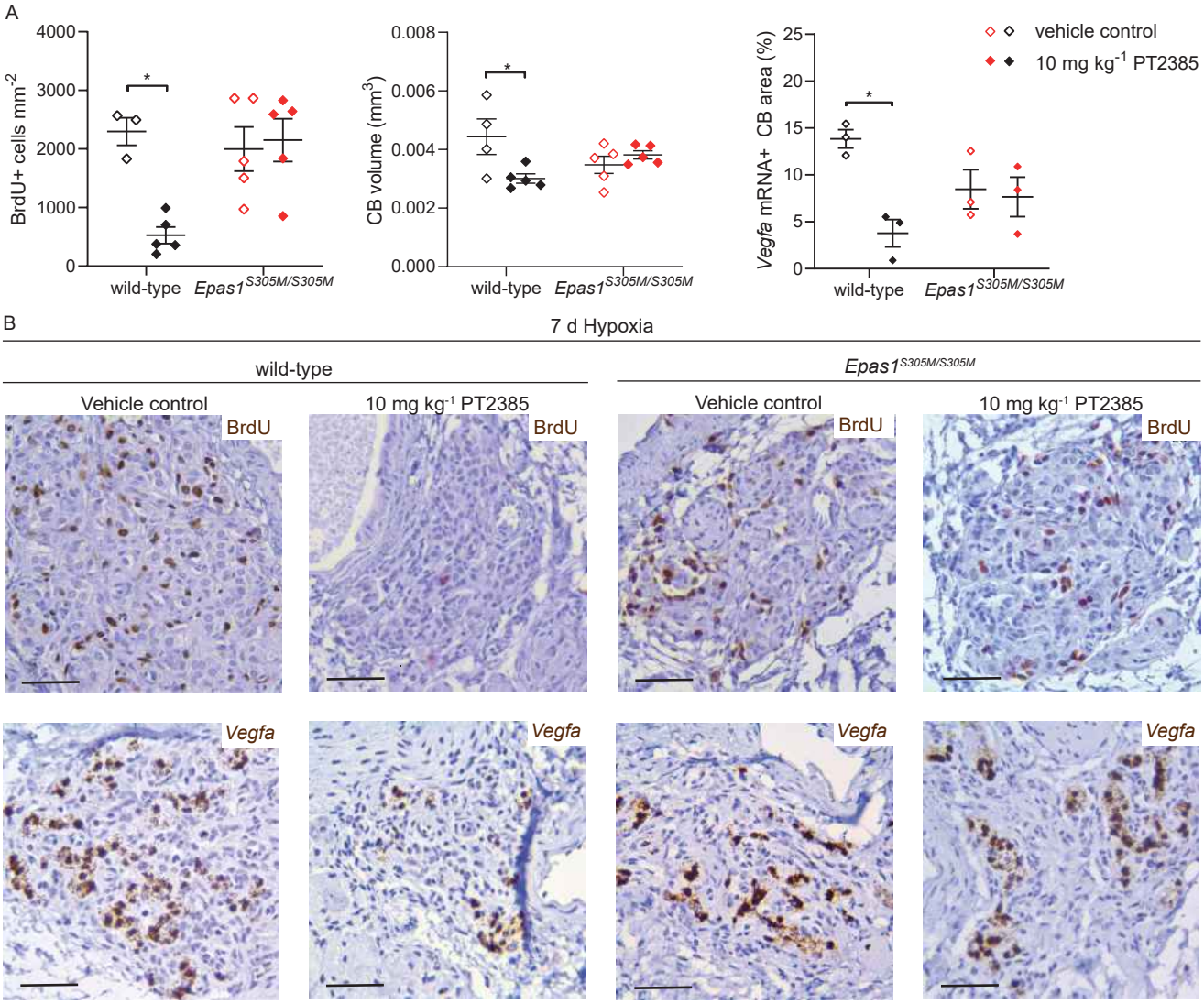

Figure 7. Effects of PT2385 on cellular responses to hypoxia in carotid bodies of *Epas1*$^{S305M/S305M}$ male mice.

(**A**) Morphometry and (**B**) representative images of carotid bodies (CBs) from wild-type and *Epas1*$^{S305M/S305M}$ mice treated twice daily with 10 mg kg^{-1} PT2385 (or vehicle) beginning 24 h before and continuing throughout 7 d exposure to hypoxia (10 % oxygen)(to a total of 8 d treatment). (**A**) Quantification of BrdU+ cells per mm^2 (left panel), CB volumes (middle panel), *Vegfa* mRNA+ CB area (right panel). Data were analysed by two-way ANOVAs followed by Holm-Sidak's multiple comparisons two-tailed tests, for which significance is reported in the graphs, * $P < 0.05$. (**B**) Immunostaining for BrdU and in situ hybridisation for *Vegfa* mRNA. Scale bars represent 50 μm.

Tables

Table 1. Effect of PT2385 on ventilatory acclimatisation to hypoxia in wild-type male mice.

		AVR (mL min^{-1} g^{-1})							
		3 mg kg^{-1} PT2385				10 mg kg^{-1} PT2385			
		Vehicle control		3 mg kg^{-1} PT2385		Vehicle control		10 mg kg^{-1} PT2385	
	Time-point	Mean	SEM	Mean	SEM	Mean	SEM	Mean	SEM
10 % O_2	Baseline	0.14	± 0.61	-0.24	± 0.97	0.77	± 0.55	-0.12	± 0.63
	2 d H	2.28	± 0.66	0.49	± 0.89	2.18	± 0.51	0.60	± 0.27
	5 d H	2.14	± 0.79	0.36	± 0.66	2.89	± 0.38	0.59	± 0.29
	7 d H	3.07	± 0.46	1.02	± 0.43	3.32	± 0.66	0.18	± 0.39
	ANOVA *P* value	***0.006***			*0.979*	***<0.001***			*0.073*
10 % O_2 / 3 % CO_2	Baseline	4.35	± 0.91	4.18	± 0.43	4.84	± 0.87	4.31	± 0.73
	2 d H	7.31	± 1.16	2.65	± 0.31	8.57	± 0.89	2.75	± 0.29
	5 d H	8.47	± 1.75	4.03	± 0.86	9.42	± 1.03	2.39	± 0.35
	7 d H	9.22	± 1.60	4.24	± 0.90	9.08	± 1.00	2.02	± 0.62
	ANOVA *P* value	***0.002***			*0.977*	***<0.001***			*0.366*
3 % CO_2	Baseline	4.18	± 0.63	3.66	± 1.03	3.63	± 0.54	4.46	± 0.60
	2 d H	3.59	± 0.79	1.25	± 0.35	3.30	± 0.51	1.90	± 0.36
	5 d H	4.69	± 0.72	1.65	± 0.58	2.17	± 0.38	2.16	± 0.22
	7 d H	4.16	± 0.37	2.69	± 0.49	3.05	± 0.52	1.89	± 0.50
	ANOVA P value	***0.010***			*0.274*	*0.054*			*0.200*

Acute ventilatory responses (AVRs) of wild-type male mice before (Baseline) and following twice daily treatment with 3 mg kg^{-1} or 10 mg kg^{-1} PT2385 (or vehicle), beginning 24 h before 7 d hypoxia (H, 10 % oxygen) and continuing throughout (to a total of 8 d treatment). Two-way repeated measures ANOVAs (right hand column *P* value = time factor; bottom row *P* value = drug factor; right column, bottom row *P* value = time/ drug interaction factor), with the Baseline (prior to PT2385) recordings excluded from statistical analysis; $n = 4$ for 3 mg kg^{-1}, $n = 6$ for 10 mg kg^{-1}. $P < 0.05$ comparisons are highlighted in bold.

Table 2. Effect of PT2385 on ventilatory acclimatisation to hypoxia in wild-type and *Epas1*$^{S305M/S305M}$ male mice.

		AVR (mL min^{-1} g^{-1})							
		wild-type				*Epas1* $^{S305M/S305M}$			
	Time-point	Vehicle control Mean	Vehicle control SEM	10 mg kg^{-1} PT2385 Mean	10 mg kg^{-1} PT2385 SEM	ANOVA *P* value	Vehicle control Mean	Vehicle control SEM	10 mg kg^{-1} PT2385 Mean	10 mg kg^{-1} PT2385 SEM	ANOVA *P* value
10% O_2	Baseline	0.13	± 0.47	-0.62	± 0.40		-1.16	± 0.70	0.12	± 0.32	
	2 d H	2.43	± 0.25	1.08	± 0.52		1.53	± 0.61	0.99	± 0.56	
	5 d H	2.73	± 0.35	0.84	± 0.45	*0.830*	1.61	± 0.58	2.47	± 0.52	*0.121*
	7 d H	3.03	± 0.42	0.14	± 0.63		2.08	± 0.30	2.00	± 0.53	
	ANOVA *P* value	***0.001***				*0.113*	*0.889*				*0.253*
10% O_2 / 3% CO_2	Baseline	3.98	± 0.64	4.45	± 0.27		3.73	± 0.44	4.33	± 0.28	
	2 d H	7.00	± 0.77	5.04	± 0.54		7.53	± 0.63	6.85	± 0.87	
	5 d H	9.39	± 0.79	5.40	± 0.88	*0.144*	8.11	± 0.71	6.56	± 0.92	*0.821*
	7 d H	9.11	± 0.72	4.05	± 0.88		7.04	± 0.47	8.02	± 1.33	
	ANOVA *P* value	***<0.001***				*0.087*	*0.700*				*0.080*
3% CO_2	Baseline	2.33	± 0.58	2.60	± 0.55		2.69	± 0.66	1.22	± 0.64	
	2 d H	2.31	± 0.70	1.44	± 0.37		2.71	± 0.84	2.40	± 0.54	
	5 d H	3.47	± 0.49	2.73	± 0.74	*0.058*	2.87	± 0.38	2.49	± 0.32	*0.450*
	7 d H	2.77	± 0.37	2.31	± 0.44		2.67	± 0.22	1.43	± 0.35	
	ANOVA *P* value	*0.212*				*0.913*	*0.062*				*0.641*

Acute ventilatory responses (AVRs) of wild-type and *Epas1*$^{S305M/S305M}$ male mice before (Baseline) and following twice daily treatment with 10 mg kg^{-1} PT2385 (or vehicle), beginning 24 h before 7 d hypoxia (H, 10 % oxygen) and continuing throughout (to a total of 8 d treatment). Two-way repeated measures ANOVAs within each genotype group (right hand column *P* value = time factor; bottom row *P* value = drug factor; right column, bottom row *P* value = time/ drug interaction factor), with the Baseline (prior to PT2385) recordings excluded from statistical analysis; $n = 7$ for each drug/ genotype group. $P < 0.05$ comparisons are highlighted in bold.